JOURNAL OF MATERIALS SCIENCE 21 (1986) 2067–2072

Sintering behaviour of powder compacts with multiheterogeneities

CHUN-HWAY HSUEH
Department of Materials Science and Mineral Engineering, University of California, Berkeley, California 94720, USA

The sintering behaviour of a powder compact containing uniformly distributed heterogeneities has been analysed. The results reveal a strong retardation of sintering in the presence of non-sinterable agglomerates, due to the development of a uniform hydrostatic tensile stress in the powder matrix. The variation in stresses and sintering rate depends strongly on the total volume fraction of heterogeneities especially when the volume fraction is small, but is insensitive to the actual number of heterogeneities. Specific results are calculated using densification and deformation laws pertinent to Al_2O_3.

1. Introduction

Heterogeneities in a green compact typically sinter at different rates than the host powder and thereby exert several influences on the sintering body. In particular, stresses develop in association with the differential shrinkage characteristics of the heterogeneity. The stresses may cause sintering damage, such as crack-like flaws, planar array of voids or isolated pores [1–4]. Additionally, residual stresses may remain after densification. Both effects tend to limit the mechanical strength of the sintered body. The heterogeneities also influence the net sintering rate of the compact. Some of the important trends in stress development and sintering rates have recently been determined for isolated heterogeneities [5] and multiheterogeneities with finite volume fraction [6, 7]. Distinction between the two models concerns the differing tendency toward the development of hydrostatic stress. Appreciable hydrostatic stress develops in the matrix as the volume fraction of heterogeneities increases. Furthermore, when the heterogeneities have lower sintering rates than the matrix, the hydrostatic stress in the matrix is tensile in nature, whereupon the sintering rate is profoundly reduced.

The model for the multiheterogeneity problem [7] was based on the premise that the volume fraction of heterogeneities is small (< 0.1). As a complement to the previous studies [5, 7], an analysis dealing with an explicit number of heterogeneities having finite volume fraction is considered in the present study. To achieve this, a single heterogeneity in the host with finite volume fraction is considered first and then extended to larger numbers of heterogeneities. The present analysis deals specifically with non-sinterable heterogeneities, typically hard agglomerates, but the method is general and can be applied to any initial heterogeneity.

2. Stress analysis

To solve the stress distribution in a powder compact, it is necessary to choose a simple model, which retains the essential features of the problem. The model chosen in the present study assumes the heterogeneity is spherical, and is large enough for the powder matrix to be viewed as a continuum solid. Thus, the analysis can be based upon a continuum solution of a misfitting inclusion in a matrix [8].

2.1. Single heterogeneity

As shown in Fig. 1a, the spherical heterogeneity is assumed to have a radius, a, and the powder matrix surrounding the heterogeneity has an outer radius, b. The volume fraction of the heterogeneity, f, is given by

$$f = \left(\frac{a}{b}\right)^3 \tag{1}$$

The powder compact is susceptible to viscoelastic deformation during sintering. Thus, stress development during sintering is treated as a viscoelastic problem, wherein the elastic streses are first assessed and then transformed into the time dependent viscoelastic solution [5–7]. The elastic stresses are determined by the procedure of firstly allowing the two constituents to exhibit an unconstrained differential shrinkage. Then, equal but opposite radial tractions, σ, are placed around the surfaces in order to restore displacement continuity at the interface. For a spherical zone, the solution is well known. Nevertheless, the essential procedural steps are briefly described.

The radial and hoop stresses within the spherical heterogeneity subject to the surface traction, σ, is given by [9]

$$\sigma_r(r) = \sigma_\theta(r) = \sigma_\phi(r) = \sigma \tag{2}$$

while the corresponding stresses in the matrix are [9]

$$\sigma_r(r) = \frac{\sigma a^3(b^3 - r^3)}{r^3(b^3 - a^3)} \tag{3a}$$

$$\sigma_\theta(r) = \sigma_\phi(r) = -\frac{\sigma a^3(2r^3 + b^3)}{2r^3(b^3 - a^3)} \tag{3b}$$

where r is the distance from the centre of the compact

0022–2461/86 $03.00 + .12

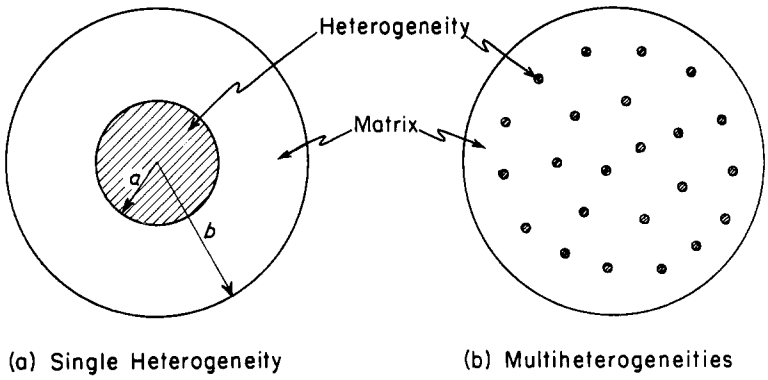

Figure 1 Schematic showing (a) a single spherical heterogeneity, and (b) n unisized heterogeneities distributed uniformally in the powder compact.

and θ, ϕ are the polar and azimuthal angles, respectively. Furthermore, the hydrostatic stresses in the heterogeneity, σ_h, and the matrix, σ_m, can be derived from Equations 2 and 3 such that

$$\sigma_h(r) = \sigma \tag{4a}$$

$$\sigma_m(r) = -\sigma f/(1-f) \tag{4b}$$

It is noted that the hydrostatic stresses are uniform in both the heterogeneity and the matrix (Equation 4) and satisfy the relation

$$\sigma_h f + \sigma_m(1-f) = 0 \tag{5}$$

The interface stress, σ, and hence the hydrostatic stress σ_h and σ_m are dictated by the boundary conditions,as shown in the following.

The total strain within the heterogeneity is the sum of the elastic and the shrinkage strains, such that,

$$\varepsilon_\theta^h = \frac{\sigma(1-2\nu_h)}{E_h} + \varepsilon_h \tag{6}$$

where E_h and ν_h are the Young's modulus and Poisson's ratio, respectively, and ε_h is the shrinkage strain due to sintering of the heterogeneity. Similarly, the total strain within the matrix can be expressed as

$$\varepsilon_\theta^m(r) = \frac{-\sigma a^3}{2E_m r^3(b^3-a^3)} \times [2r^3 + b^3 + \nu_m(b^3-4r^3)] + \varepsilon_m \tag{7}$$

The interface traction, σ, can be determined from the strains, subject to the requirements that the displacements be continuous at the interface

$$u_r^h(r) = u_r^m(r) \qquad (r=a) \tag{8a}$$

such that

$$\varepsilon_\theta^h(r) = \varepsilon_\theta^m(r) \qquad (r=a) \tag{8b}$$

Substitution of Equations 6 and 7 into Equation 8b yields

$$\sigma = (\varepsilon_m - \varepsilon_h)\Big/\left(\frac{1}{3K_h} + \frac{1}{4G_m}\frac{1}{1-f} + \frac{1}{3K_m}\frac{f}{1-f}\right) \tag{9}$$

where K and G are the bulk and shear moduli, respectively. In the case of non-sinterable hard heterogeneities [10], wherein $\varepsilon_h = 0$ and $K_h \to \infty$, Equation 9 reduces to

$$\sigma = [\varepsilon_m(1-f)]\Big/\left(\frac{1}{4G_m} + \frac{f}{3K_m}\right) \tag{10}$$

and the hydrostatic stresses in the heterogeneity and matrix can be derived from Equations 4 and 10 such that

$$\sigma_h = [\varepsilon_m(1-f)]\Big/\left(\frac{1}{4G_m} + \frac{f}{3K_m}\right) \tag{11a}$$

$$\sigma_m = -\varepsilon_m f\Big/\left(\frac{1}{4G_m} + \frac{f}{3K_m}\right) \tag{11b}$$

2.2. Multiheterogeneities

The single heterogeneity is subdivided into n equal-sized heterogeneities with volume fraction f/n for each individual heterogeneity and distributed uniformly in the powder compact (Fig. 1b). The stress distribution in the multiheterogeneity problem is complex, and a rigorous stress analysis requires extensive numerical computation. An approximate solution is thus suggested, which permits both the identification of the important multiheterogeneity effects and elucidates the essential trends. To achieve this, it is assumed that the effect of the location of the heterogeneity and of the interaction between heterogeneities can be ignored. The hydrostatic stress in the matrix derived from each individual heterogeneity, σ_{ml}, is thus

$$\sigma_{ml} = (-\varepsilon_m f/n)\Big/\left(\frac{1}{4G_m} + \frac{1}{3K_m}\frac{f}{n}\right) \tag{12}$$

and the resultant hydrostatic stress in the matrix due to the n heterogeneities is

$$\sigma_m = -\varepsilon_m f\Big/\left(\frac{1}{4G_m} + \frac{1}{3K_m}\frac{f}{n}\right) \tag{13a}$$

while the corresponding hydrostatic stress in heterogeneity is

$$\sigma_h = [\varepsilon_m(1-f)]\Big/\left(\frac{1}{4G_m} + \frac{1}{3K_m}\frac{f}{n}\right) \tag{13b}$$

These elastic stresses are converted into the equivalent viscoelastic stresses in the following section.

2.3. Viscoelastic stresses

The viscoelastic stress determinations adopt the usual assumptions that the deformation satisfies a Maxwell model. The viscoelastic stress can be determined from the elastic stress by applying Laplace and inverse Laplace transforms [7], such that the viscoelastic hydrostatic stress in heterogeneities and matrix are

$$\sigma_h(t) = \int_0^t \frac{12K_mG_m(1-f)}{3K_m + 4G_m f/n}\dot{\varepsilon}_m \times \exp\left[\frac{-3K_mG_m(t-u)}{(3K_m + 4G_m f/n)\eta_m}\right]du \tag{14a}$$

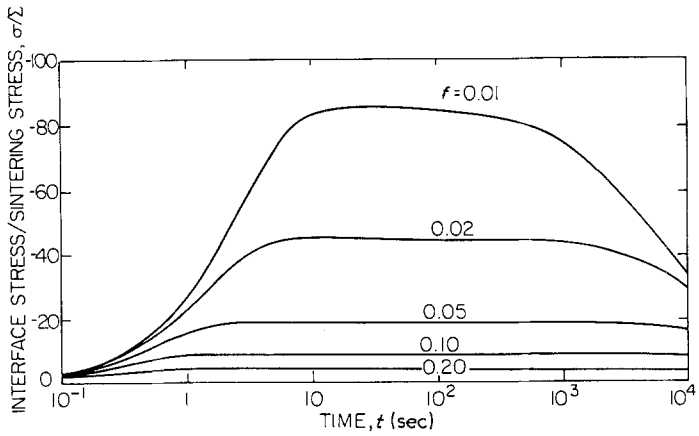

Figure 2 Plot of normalized interface stress as a function of time at different volume fraction of heterogeneities, f, for $\varrho_0^m/\varrho_f = 0.5$ and $n \to \infty$.

and

$$\sigma_m(t) = \int_0^t \frac{-12K_mG_mf}{3K_m + 4G_mf/n}\dot{\varepsilon}_m \times \exp\left[\frac{-3K_mG_m(t-u)}{(3K_m + 4G_mf/n)\eta_m}\right]du \quad (14b)$$

where t and η are time and viscosity, respectively. Furthermore, when the volume fraction of the heterogeneities, f, is small or the number, n, is large, Equation 14 can be simplified to

$$\sigma_h(t) = \int_0^t 4G_m(1-f)\dot{\varepsilon}_m \exp\left[-G_m(t-u)/\eta_m\right]du \quad (15a)$$

$$\sigma_m(t) = \int_0^t -4G_mf\dot{\varepsilon}_m \exp\left[-G_m(t-u)/\eta_m\right]du \quad (15b)$$

Determination of the residual stress is thus contingent upon the shrinkage rate of the matrix, $\dot{\varepsilon}_m$, as well as the parameters G_m, K_m and η_m. Stress solutions may thus be obtained by incorporating density dependent constitutive laws for each of these variables into Equations 14 and 15 and integrating. Specific results obtained for Al_2O_3 are presented in the subsequent section, using a finite difference scheme.

2.4. Constitutive laws

The various constitutive laws describing the behaviour of the porous sintering body have previously been established using formulae based on models of sintering and creep in conjunction with typically encountered experimental characteristics [5].

$$\dot{\varrho}/\varrho_f = \frac{\beta}{\tau}\frac{(1-\varrho/\varrho_f)^{1+1/\beta}}{(1-\varrho_0/\varrho_f)^{1/\beta}}(1-\sigma_m/\Sigma) \quad (16a)$$

$$\eta = A(\varrho/\varrho_f)^{\delta}(1-\varrho/\varrho_f)^{-1/\beta} \quad (16b)$$

$$G = G_0\{1 + B(1-\varrho/\varrho_f)[1-(B+1) \times (1-\varrho/\varrho_f)]^{-1}\} \quad (16c)$$

$$K = K_0\{1 + B(1-\varrho/\varrho_f)[1-(B+1) \times (1-\varrho/\varrho_f)]^{-1}\} \quad (16d)$$

$$\dot{\varepsilon} = -\dot{\varrho}/3\varrho \quad (16e)$$

where ϱ_0 and ϱ_f are the initial and final densities, respectively, Σ is the sintering stress and β, τ, δ, A and B are coefficients obtained by fitting Equation 16 to experimental data. Data for Al_2O_3 are used for present purposes (Table I) [5].

3. Results

Heterogeneities with limited sinterability substantially reduce the net sintering rate of the compact, because compressive stress develops at the interface when the powder matrix sinters and shrinks, which in turn induces hydrostatic tension in the powder matrix (Equation 4b) and opposes the sintering stress (Equation 16a).

The trends in the interface stress induced by a large number of non-sinterable heterogeneities (Equation 15a) are plotted in Fig. 2. Evidently, the peak stress diminishes and persists for longer times as the volume fraction of the heterogeneities increases. The specific variation in the peak interface stress with volume fraction of heterogeneities is plotted in Fig. 3. The corresponding peak hydrostatic tension in the powder matrix is plotted in Fig. 4. It is noted that the hydrostatic tension is limited by the sintering stress of the powder matrix because sintering stops when the hydrostatic tension approaches the sintering stress. The opposite trends in σ_h and σ_m with respect to f (Figs 3 and 4) arise because these stresses are interrelated through f, as expressed by Equation 5, such that $\sigma_m \to 0$ as $f \to 0$.

Specific trends in the density with time and heterogeneity concentration are illustrated in Fig. 5. It is evident that the sintering rates are substantially reduced by the heterogeneities, even when f is small (i.e. of order 0.01) as observed experimentally [10], where the density of the powder compact of ZnO, with initial grain size $\sim 0.4\,\mu m$ and sintered at 700° C, were drastically reduced by the addition of uniformly dispersed, hard and coarse-grained ($\sim 12\,\mu m$) SiC particles (Fig. 6) [10]. The effect is most pronounced for

TABLE I Parameters for Al_2O_3 at $\varrho_0/\varrho_f = 0.5$ and $T = 1500°C$

Parameter	Value
β	0.6
τ	190.5 sec
Σ	1.5 MPa
A	100 GPa sec
δ	0.5
G_0	50 GPa
K_0	130 GPa
B	−3.2

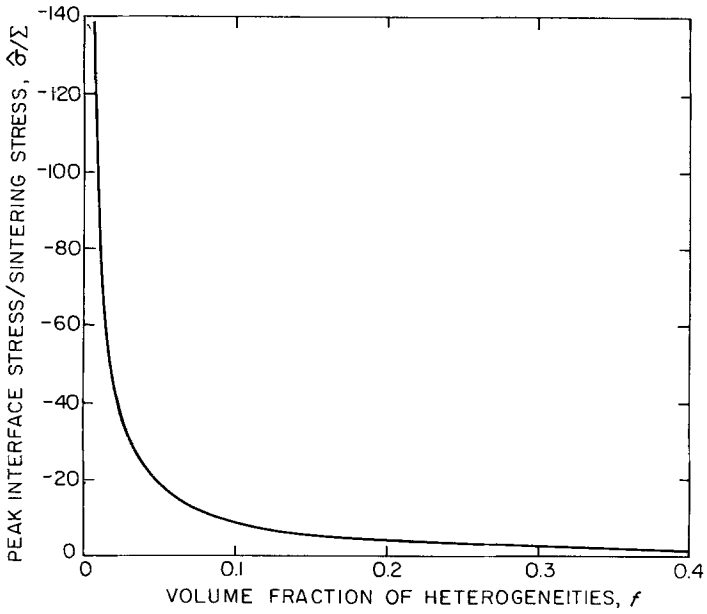

Figure 3 Plot of normalized peak interface stress as a function of volume fraction of heterogeneities for $\varrho_0^m/\varrho_f = 0.5$ and $n \to \infty$.

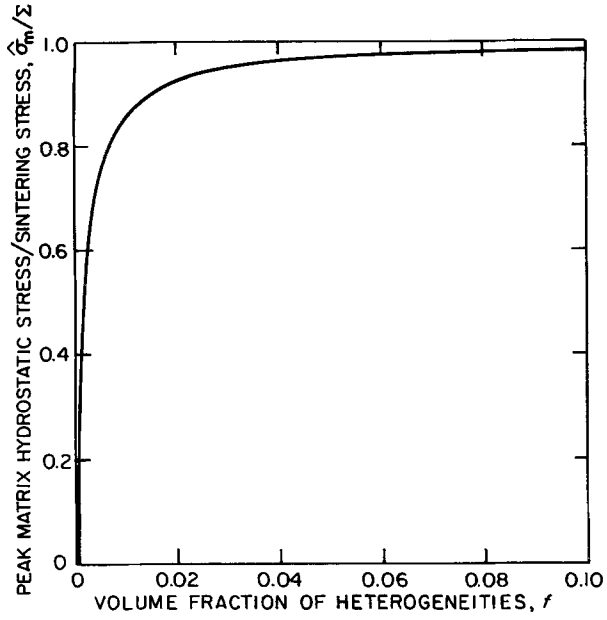

Figure 4 Plot of normalized peak matrix hydrostatic stress as a function of volume fraction of heterogeneities for $\varrho_0^m/\varrho_f = 0.5$ and $n \to \infty$.

intermediate times, as exemplified by plotting the ratio of the net density change in the matrix, $\Delta\varrho$, to the equivalent density change in the absence of heterogeneities, $\Delta\varrho_0$ (Fig. 7). Such temporal densification characteristics obtain because hydrostatic tensile stress develops after an initial period of densification (see Fig. 2), whereupon the matrix sintering rate is retarded and the densification rate exhibits an initial decrease. However, at longer time periods, the sintering rate differential diminishes and the stress tends to be relaxed by viscoelastic deformation of the matrix [5], thereby allowing the relative densification rate to increase and, eventually, approach unity (Fig. 7).

It is worthwhile to note the importance of the relationships evident in Figs 3–5 on the microstructural development of the powder compact. While the reduction of the sintering rate in the powder matrix is smaller with lower volume fraction of non-sinterable heterogeneities, it can nevertheless lead to higher interface compressive stresses, which in turn induce higher circumferential tensile stresses in the powder matrix (Equation 3) and cause sintering damage. Conversely, higher volume fraction of non-sinterable

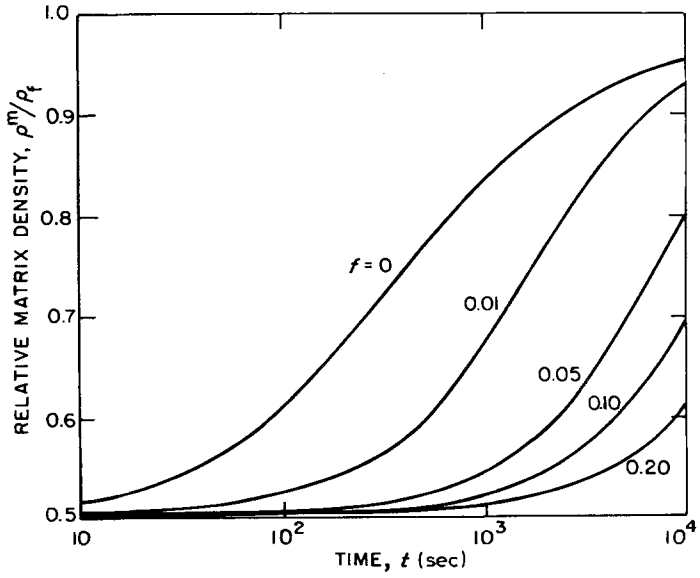

Figure 5 Plot of relative matrix density as a function of time at different volume fraction of heterogeneities, f, for $\varrho_0^m/\varrho_f = 0.5$ and $n \to \infty$.

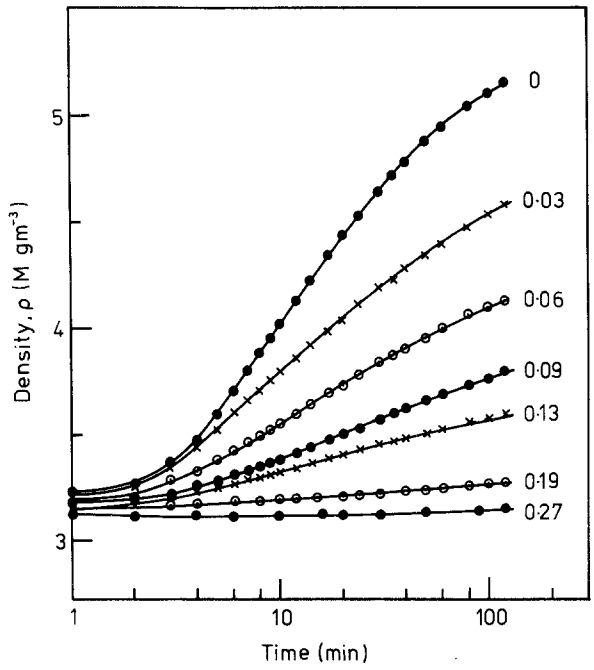

Figure 6 Density as a function of time for ZnO containing different volume fraction of SiC (courtesy of M. N. Rahaman).

heterogeneities leads to lower interface stress, but it severely reduces the sintering rate of the powder matrix and yields a weak, porous matrix. Consequently, close control of the heterogeneity content is important in the realization of the maximum sinterability of a powder compact.

The effects of the number of heterogeneities (with fixed total volume fraction) on the sintering behaviour of the compact are also studied. It is shown in Equation 14 that the effects can be ignored when the volume fraction, f, is small or the number, n is large. However, the hydrostatic stresses increase as n increases and the variation vanishes after an initial period of sintering, such that the peak stress is independent of n, as shown in Fig. 8. The relative density change as a function of time is shown in Fig. 9. It can be seen that the densification rate shows an initial decrease with increase in n and then become independent of n, consistent with the trends in the hydrostatic stress (Fig. 8).

4. Concluding remarks

A distribution of non-sinterable heterogeneities in a powder compact is shown to decrease the sintering

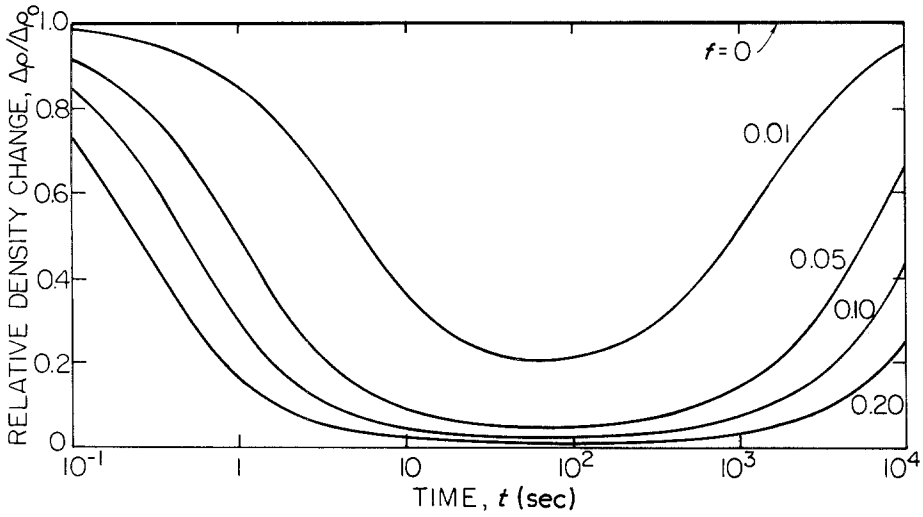

Figure 7 Plot of relative density change as a function of time at different volume fraction of heterogeneities, f, for $\varrho_0^m/\varrho_f = 0.5$ and $n \to \infty$.

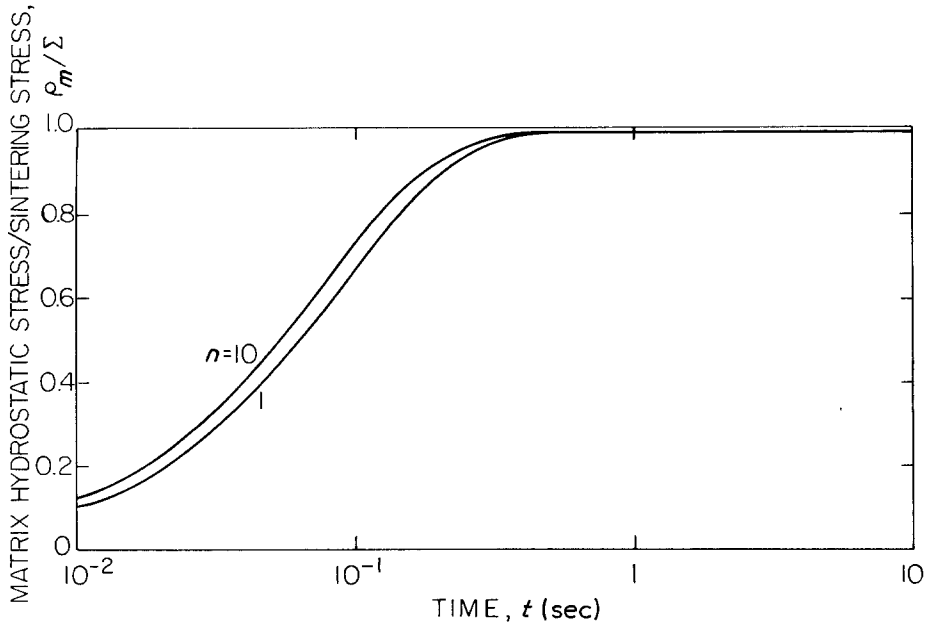

Figure 8 Plot of normalized matrix hydrostatic stress as a function of time for number of heterogeneities, n, equals 1 and 10, $f = 0.4$ and $\varrho_0^m/\varrho_f = 0.5$.

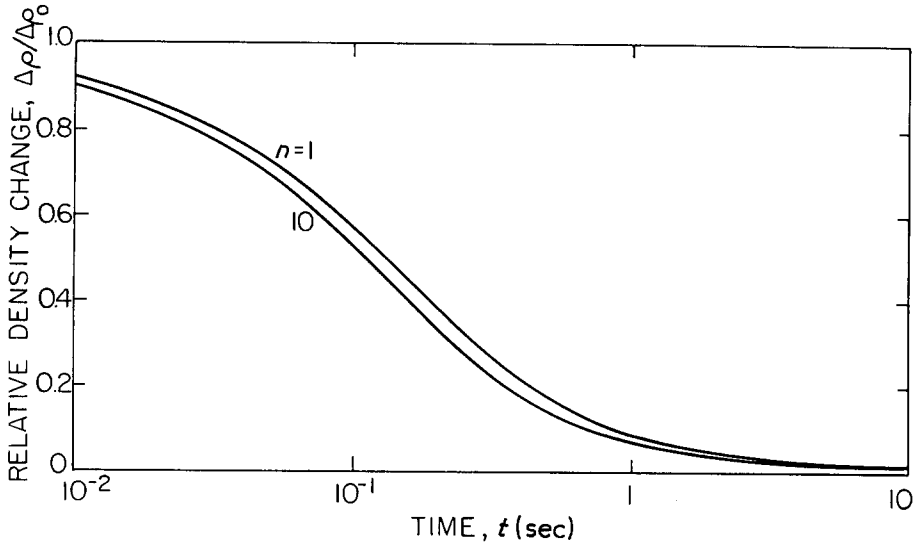

Figure 9 Plot of relative density change as a function of time for number of heterogeneities, n, equals 1 and 10, $f = 0.4$ and $\varrho_0^m/\varrho_f = 0.5$.

rate by inducing hydrostatic tensile stresses in the powder matrix. The effects are most pronounced at relatively small volume fractions, f, of heterogeneities. The actual number of heterogeneities, n, influences the sintering behaviour only during the initial period, such that the hydrostatic tensile stress increases and the sintering rate decreases with increase in n. Furthermore, the effects of n on stresses and sintering rate can be ignored for small volume fractions or for a large number of heterogeneities.

The specific results generated in the present study are for Al_2O_3 powder matrix containing non-sinterable heterogeneities. However, the procedure is general in nature and can be used to predict sintering behaviour of any powder compact containing heterogeneities, by using Equation 14 and incorporating density dependent constitutive laws for each variable. The trends revealed in this study are expected to be obtained for other materials, albeit that the specific stress levels must be material dependent. Improved computations await additional sintering and creep rate data.

Acknowledgements

The author would like to thank Professors A. G. Evans and L. C. De Jonghe for their helpful comments. This work was supported by the Director, Office of Energy Research, Office of Basic Energy Sciences, Materials Science Division of the US Department of Energy under Contract No. DE-AC03-76SF00098.

References

1. A. G. EVANS, *J. Amer. Ceram. Soc.* **65** (1982) 497.
2. K. D. REEVE, *Amer. Ceram. Soc. Bull.* **42** (1962) 452.
3. F. F. LANGE and M. METCALF, *J. Amer. Ceram. Soc.* **66** (1983) 398.
4. F. W. DYNYS and J. W. HOLLORAN, *ibid.* **67** (1984) 596.
5. C. H. HSUEH, A. G. EVANS, R. M. CANNON and R. J. BROOK, *Acta Metall.* in press.
6. R. RAJ and R. K. BORDIA, *ibid.* **32** (1984) 1003.
7. C. H. HSUEH, A. G. EVANS and R. M. McMEEKING, *J. Amer. Ceram. Soc.* in press.
8. J. D. ESHELBY, *Proc. R. Soc.* **214a** (1957) 376.
9. S. P. TIMOSHENKO and J. N. GOODIER, "Theory of Elasticity" (McGraw-Hill, New York, 1951) p. 394.
10. L. C. De JONGHE, M. N. RAHAMAN and C. H. HSUEH, *Acta Metall.* in press.

Received 25 March
and accepted 14 August 1985